Free vibration of thin-walled composite beams with static initial stresses and deformations

Sebastián P. Machado*, Víctor H. Cortínez

Grupo Análisis de Sistemas Mecánicos, Facultad Regional Bahía Blanca, Universidad Tecnológica Nacional, 11de abril 461, B8000LMI Bahía Blanca, Argentina
CONICET, Argentina

Abstract

The influence of the initial in-plane deformations, generated by the action of a static external loading, as well as the effect of shear flexibility on the dynamic behavior of bisymmetric thin-walled composite beams has been investigated in this paper. The analysis is based on a geometrically non-linear theory based on large displacements and rotations. The Ritz variational method is used in order to discretize the governing equation and an analytical method is used to obtain the natural frequencies. In the investigation open cross-section beams subjected to initial uniform moment, distributed load and concentrated load are considered. The numerical results show that when the ratio of the smaller axis flexural stiffness to the major axis flexural stiffness is large, classic analysis of vibration may lead to inaccurate predictions because of the effects of initial displacements. Besides, the effects of span length and height of the load point have also been investigated for different laminate stacking sequences.
© 2006 Elsevier Ltd. All rights reserved.

Keywords: Thin-walled beams; Shear flexibility; Composite material

1. Introduction

Thin-walled beam structures made of advanced anisotropic composite materials are increasingly found in the design of the aircraft wings, helicopter blades, axles of vehicles and so on, due to their outstanding engineering properties, such as high strength/stiffness to weight ratios and favorable fatigue characteristics. The interesting possibilities provided by fiber reinforced composite materials can be used to enhance the response characteristics of such structures that operate in complex environmental conditions. Since composite thin-walled beam members are widely used in aerospace, automobile and civil architecture industries, it is important to ensure that their design is reliable and safe.

There are several studies about the dynamic behavior of thin-walled isotropic beams subjected to an initial stress static state. For example, Vlasov [1] examined in detail

the problem of vibrations of thin-walled beams subjected to a longitudinal load located in one of their ends. Then, Bolotin [2] considered the study of a simply supported beam subjected to an axial or transverse load. In both studies the effect of shear deformation was not considered. Coulter and Miller [3] investigated the vibration of tapered plane cross-section beams subject to distributed axial forces. Cortínez and Rossi [4] studied the dynamics of shear deformable thin-walled open beams, subjected to an axial initial stress state. They obtained natural frequencies of vibration by means of the finite elements method based on a linear formulation. Kim et al. [5] presented an improved second-order formulation in which the transverse shear effect was ignored. They analyzed the free vibration of thin-walled tapered beams subjected to an axial load. The dynamic response of non-symmetrical thin-walled beams subjected to concentrated and distributed axial loads was analyzed by Jun et al. [6] by means of a Bernoulli–Euler beam theory. They studied the warping effect and the flexural–torsional coupling of cantilever beams. On the other hand, Mohri et al. [7] presented a higher-order non shear deformable model to investigate the dynamic behavior of thin-walled open sections in the pre- and post-buckling state.

* Corresponding author at: Grupo Análisis de Sistemas Mecánicos, Facultad Regional Bahía Blanca, Universidad Tecnológica Nacional, 11de abril 461, B8000LMI Bahía Blanca, Argentina. Tel.: +54 0291 4555220; fax: +54 0291 4555311.

E-mail addresses: smachado@frbb.utn.edu.ar (S.P. Machado), vcortine@frbb.utn.edu.ar (V.H. Cortínez).

In their numeric examples they considered simply supported beams subjected to axial and distributed transverse loads.

In spite of the practical interest and future potential of composite beam structures, particularly in the context of aerospace and mechanical applications, the quantity of available investigations devoted to studying the dynamic response behavior of composite beams subjected to an initial stress state is relatively limited. Cortínez and Piovan [8] developed a linear theoretical model for thin-walled beams of open and closed cross-section. In their work they studied the effect of the initial state of stresses on the natural frequencies of the structure. Also, they analyzed the influence of shear deformation when the fibers are oriented in the longitudinal direction of the beam. Jun et al. [9] studied the dynamic flexural–torsional response of axially loaded beams, by means of a Timoshenko model [10] for thin-walled beams of closed section.

It should be emphasized here that the necessity of incorporating transverse shear effect arises from the fact that the advanced fiber composite materials exhibit high flexibilities in transverse shear [11,8].

On the other hand, the effect of large displacement (associated to an initial static state of deformation) on the dynamic behavior of thin-walled composite beams has not been yet studied. Machado and Cortínez [12] investigated the influence of initial displacements on the lateral buckling behavior of thin-walled composite beams. Their numerical results show that the classical predictions of lateral buckling are conservative when the pre-buckling displacements are not negligible.

The primary purpose of this paper is to investigate numerically the effects of the initial displacements as well as the effect of shear deformation on the dynamic response of bisymmetric thin-walled composite beams subjected to initial uniform moment, distributed load and concentrated load. Simply supported, cantilever and fixed-end beams are considered.

A second purpose is to investigate the effects of the span length and the load height on the dynamic behavior considering different laminate stacking sequences.

The analysis is based in a geometrically non-linear shear deformable beam theory recently developed by the authors [12] that is valid for symmetric balanced and especially orthotropic laminates [13,14].

In order to solve the governing equations, the Ritz method [15] is used for reducing the variational problem to an algebraic equation for determining the natural frequencies of vibration. The results obtained are compared with values obtained by means of the linearized theory, with the purpose of evaluating the importance of the effects considered in the present model. Besides, numerical solutions are compared with solutions by Abaqus's shell element in order to show the practical usefulness of this formulation.

2. Kinematics

A straight thin-walled composite beam with an arbitrary cross-section is considered (Fig. 1). The points of the structural
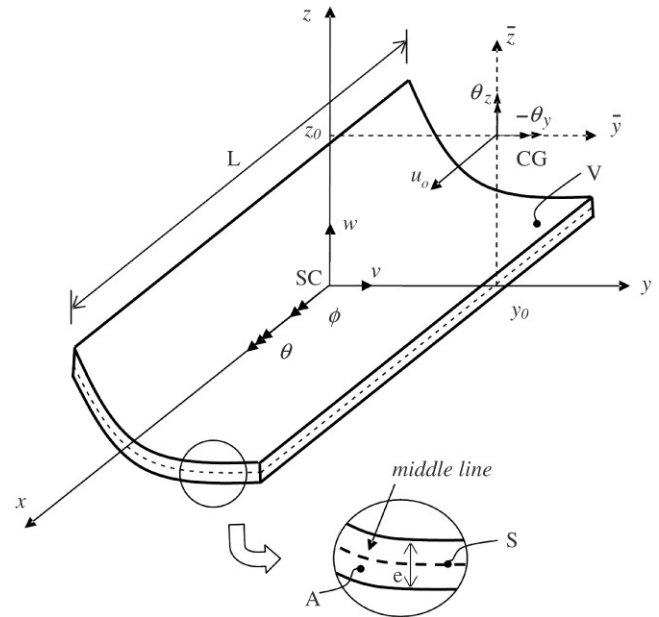

Fig. 1. Coordinate system of the cross-section and notation for displacement measures.

member are referred to a Cartesian coordinate system $(x, \bar{y}, \bar{z})$, where the x-axis is parallel to the longitudinal axis of the beam while $\bar{y}$ and $\bar{z}$ are the principal axes of the cross-section. The axes y and z are parallel to the principal ones but have their origin at the shear center (defined according to Vlasov's theory of isotropic beams). The coordinates corresponding to points lying on the middle line are denoted as Y and Z (or $\bar{Y}$ and $\bar{Z}$). In addition, a circumferential coordinate s and a normal coordinate n are introduced on the middle contour of the cross-section.

$$\bar{y}(s, n) = \bar{Y}(s) - n\frac{dZ}{ds}, \qquad \bar{z}(s, n) = \bar{Z}(s) + n\frac{dY}{ds} \qquad (1)$$

$$y(s, n) = Y(s) - n\frac{dZ}{ds}, \qquad z(s, n) = Z(s) + n\frac{dY}{ds}. \qquad (2)$$

On the other hand, y_0 and z_0 are the centroidal coordinates measured with respect to the shear center.

$$\bar{y}(s, n) = y(s, n) - y_0$$
$$\bar{z}(s, n) = z(s, n) - z_0. \qquad (3)$$

The present structural model is based on the following assumptions [8]:

(1) The cross-section contour is rigid in its own plane.
(2) The warping distribution is assumed to be given by the Saint-Venant function for isotropic beams.
(3) Flexural rotations (about the $\bar{y}$ and $\bar{z}$ axes) are assumed to be moderate, while the twist ϕ of the cross-section can be arbitrarily large.
(4) Shell force and moment resultants corresponding to the circumferential stress σ_{ss} and the force resultant corresponding to γ_{ns} are neglected.
(5) The curvature at any point of the shell is neglected.

(6) Twisting linear curvature of the shell is expressed according to the classical plate theory.

(7) The laminate stacking sequence is assumed to be symmetric and balanced, or especially orthotropic [13,14].

According to these hypotheses the displacement field is assumed to be in the following form:

$$u_x = u_o - \bar{y}(\theta_z \cos\phi - \theta_y \sin\phi) - \bar{z}(\theta_y \cos\phi - \theta_z \sin\phi)$$
$$+ \omega \left[\theta - \frac{1}{2}(\theta'_y \theta_z - \theta_y \theta'_z) \right] + (\theta_z z_0 - \theta_y y_0)\sin\phi$$

$$u_y = v - z\sin\phi - y(1 - \cos\phi) - \frac{1}{2}(\theta_z^2 \bar{y} + \theta_z \theta_y \bar{z})$$

$$u_z = w + y\sin\phi - z(1 - \cos\phi) - \frac{1}{2}(\theta_y^2 \bar{z} + \theta_z \theta_y \bar{y}). \tag{4}$$

This expression is a generalization of others previously proposed in the literature as explained in [12].

In the above expressions ϕ, θ_y and θ_z are measures of the rotations about the shear center axis, $\bar{y}$ and $\bar{z}$ axes, respectively; θ represents the warping variable of the cross-section. Furthermore the superscript 'prime' denotes derivation with respect to the variable x.

The components of the Green's strain tensor which incorporates the large displacement are obtained as explained in [12].

3. Variational formulation

Taking into account the adopted assumptions, the principle of virtual work for a composite shell may be expressed in the form [16,8]:

$$\int\int (N_{xx}\delta\varepsilon_{xx}^{(0)} + M_{xx}\delta\kappa_{xx}^{(1)} + N_{xs}\delta\gamma_{xs}^{(0)} + M_{xs}\delta\kappa_{xs}^{(1)}$$
$$+ N_{xn}\delta\gamma_{xn}^{(0)})\mathrm{d}s\mathrm{d}x$$
$$- \int\int\int \rho(\ddot{u}_x\delta u_x + \ddot{u}_y\delta u_y + \ddot{u}_z\delta u_z)\mathrm{d}s\mathrm{d}n\mathrm{d}x$$
$$- \int\int (\bar{q}_x\delta\bar{u}_x + \bar{q}_y\delta\bar{u}_y + \bar{q}_z\delta\bar{u}_z)\mathrm{d}s\mathrm{d}x$$
$$- \int\int (\bar{p}_x\delta u_x + \bar{p}_y\delta u_y + \bar{p}_z\delta u_z)\big|_{x=0}\,\mathrm{d}s\mathrm{d}n$$
$$- \int\int (\bar{p}_x\delta u_x + \bar{p}_y\delta u_y + \bar{p}_z\delta u_z)\big|_{x=L}\,\mathrm{d}s\mathrm{d}n$$
$$- \int\int\int (\bar{f}_x\delta u_x + \bar{f}_y\delta u_y + \bar{f}_z\delta u_z)\mathrm{d}s\mathrm{d}n\mathrm{d}x = 0 \tag{5}$$

where N_{xx}, N_{xs}, M_{xx}, M_{xs} and N_{xn} are the shell stress resultants [12]. The beam is subjected to wall surface tractions $\bar{q}_x$, $\bar{q}_y$ and $\bar{q}_z$ specified per unit area of the undeformed middle surface and acting along the x, y and z directions, respectively. Similarly, $\bar{p}_x$, $\bar{p}_y$ and $\bar{p}_z$ are the end tractions per unit area of the undeformed cross-section specified at $x = 0$ and $x = L$, where L is the undeformed length of the beam. Besides $\bar{f}_x$, $\bar{f}_y$ and $\bar{f}_z$ are the body forces per unit of volume. Finally, $\bar{u}_x$, $\bar{u}_y$ and $\bar{u}_z$ denote the displacements at the middle line.

4. Constitutive equations

The constitutive equations of symmetrically balanced laminates may be expressed in the terms of shell stress resultants in the following form [13]:

$$\begin{Bmatrix} N_{xx} \\ N_{xs} \\ N_{xn} \\ M_{xx} \\ M_{xs} \end{Bmatrix} = \begin{bmatrix} \bar{A}_{11} & 0 & 0 & 0 & 0 \\ 0 & \bar{A}_{66} & 0 & 0 & 0 \\ 0 & 0 & \bar{A}_{55}^{(H)} & 0 & 0 \\ 0 & 0 & 0 & \bar{D}_{11} & 0 \\ 0 & 0 & 0 & 0 & \bar{D}_{66} \end{bmatrix} \begin{Bmatrix} \varepsilon_{xx}^{(0)} \\ \gamma_{xs}^{(0)} \\ \gamma_{xn}^{(0)} \\ \kappa_{xx}^{(1)} \\ \kappa_{xs}^{(1)} \end{Bmatrix} \tag{6}$$

with

$$\bar{A}_{11} = A_{11} - \frac{A_{12}^2}{A_{22}}, \qquad \bar{A}_{66} = A_{66} - \frac{A_{26}^2}{A_{22}},$$

$$\bar{A}_{55}^{(H)} = A_{55}^{(H)} - \frac{(A_{45}^{(H)})^2}{A_{44}^{(H)}} \tag{7}$$

$$\bar{D}_{11} = D_{11} - \frac{D_{12}^2}{D_{22}}, \qquad \bar{D}_{66} = D_{66} - \frac{D_{26}^2}{D_{22}}$$

where A_{ij}, D_{ij} and $A_{ij}^{(H)}$ are plate stiffness coefficients defined according to the lamination theory presented by Barbero [13]. The coefficient $\bar{D}_{16}$ has been neglected because of its low value for the considered laminate stacking sequence [8].

5. Principle of virtual work for thin-walled beams

Substituting the kinematics expressions and the constitutive equations into (5) and integrating with respect to s, one obtains the one-dimensional expression for the virtual work equation given by

$$L_M + L_K + L_P = 0 \tag{8}$$

where L_M, L_k and L_p represent the virtual work contributions due to the inertial, internal and external forces, respectively.

$$L_M = \int_0^L \rho \left[A\frac{\partial^2 u_0}{\partial t^2}\delta u_0 + I_z\frac{\partial^2 \theta_z}{\partial t^2}\delta\theta_z + I_y\frac{\partial^2 \theta_y}{\partial t^2}\delta\theta_y \right.$$
$$+ C_w\frac{\partial^2 \theta}{\partial t^2}\delta\theta + A\frac{\partial^2}{\partial t^2}(v - z_0\phi)\,\delta v$$
$$+ A\frac{\partial^2}{\partial t^2}(w + y_0\phi)\delta w$$
$$\left. + \frac{\partial^2}{\partial t^2}(-Az_0v + Ay_0w + I_s\phi)\delta\phi \right] \mathrm{d}x \tag{9}$$

where A is the cross-sectional area, I_z and I_y are the principal moments of inertia of the cross-section, C_w is the warping constant, I_s is the polar moment with respect to the shear center and ρ is the mean density of the laminate.

The expressions of L_k and L_p are the same as presented by the authors in [12]; in the same way the 1-D beam forces, in terms of the shell forces, have been defined in [12].

6. Free vibration analysis

The dynamic response of bisymmetric thin-walled composite beams is analyzed by taking into account the initial displacements due to the static load. In the case of lateral load in the vertical plane of the beam, the displacement components in the load plane are in the form $\{u, v, \theta_z, w, \theta_y, \phi, \theta\}^t = \{0, 0, 0, w, \theta_y, 0, 0\}^t$, that is to say, the beam deforms in the loading plane. It is reasonable to assume that the displacements in the load plane are solved by means of the linearized static theory [14]. Then these last expressions, which represent the deformed initial state of the beam, are replaced in the variational Eq. (8), and Ritz's method is used to discretize the resulting system. Assembling in a usual way, this last system can be written as

$$M \frac{\partial^2 U}{\partial t^2} + Kt U = 0 \tag{10}$$

where M denotes the mass matrix, U is the global vector of incremental displacements and Kt is the tangential matrix evaluated in the deformed initial state.

Assuming a harmonic incremental motion with frequency Ω, the Eq. (10) is reduced to an eigenvalue problem:

$$\left[-\Omega^2 M + Kt \right] U = 0. \tag{11}$$

Then, the numerical solution of this equation permits one to study the natural frequencies of vibration corresponding to the modes out of the load plane, in this case flexural–torsional modes.

6.1. Simply supported beams

The displacements corresponding to the load plane are obtained from the linearized version of Eq. (8). In fact, by neglecting all the non-linear terms in (8), and applying the variational calculus, the differential equations of equilibrium are obtained which are easily solved in a closed form in order to determine the displacements in the loading plane.

For the case of simply supported beams subjected to uniform bending, the initial displacements are given by the following expressions:

$$w = \frac{Mo}{2\widehat{EI}_y}(Lx - x^2); \qquad \theta_y = \frac{Mo}{2\widehat{EI}_y}(L - 2x). \tag{12}$$

The variational Eq. (8) is discretized by means of the following functions:

$$v = v_0(t) \sin\left(\frac{\pi}{L}x\right); \qquad \theta_z = \theta_{z_0}(t) \cos\left(\frac{\pi}{L}x\right);$$
$$\phi = \phi_0(t) \sin\left(\frac{\pi}{L}x\right); \qquad \theta = \theta_0(t) \cos\left(\frac{\pi}{L}x\right); \tag{13}$$

where $v_0(t), \theta_{z0}(t), \phi_0(t)$ and $\theta_0(t)$ are the associated displacement amplitudes which are time dependent. These relationships are commonly adopted as an approximation for modes of simply supported beams in both static and dynamics analysis [8,12].

Following the procedure explained previously it is possible to obtain the system (11), where the mass matrix is

$$M = \begin{bmatrix} \rho A & 0 & 0 & 0 \\ 0 & \rho I_z & 0 & 0 \\ 0 & 0 & \rho I_s & 0 \\ 0 & 0 & 0 & \rho C_w \end{bmatrix} \tag{14}$$

and the tangential stiffness matrix can be expressed as

$$Kt = K + K_G M_0 \tag{15}$$

where K is the linear elastic stiffness matrix and K_G it is the geometric stiffness matrix which considers the displacements corresponding to the stress initial state.

$$K = \begin{bmatrix} \frac{\widehat{GS}_y\pi^2}{L^2} & -\frac{\widehat{GS}_y\pi}{L} & 0 & 0 \\ -\frac{\widehat{GS}_y\pi}{L} & \widehat{GS}_y + \widehat{EI}_z\frac{\pi^2}{L^2} & 0 & 0 \\ 0 & 0 & (\widehat{GJ}+\widehat{GS}_w)\frac{\pi^2}{L^2} & -\frac{\widehat{GS}_w\pi}{L} \\ 0 & 0 & -\frac{\widehat{GS}_w\pi}{L} & \widehat{GS}_w + \widehat{EC}_w\frac{\pi^2}{L^2} \end{bmatrix} \tag{16}$$

$$K_G = \begin{bmatrix} 0 & 0 & 0 & 0 \\ 0 & 0 & -\left(1 - \frac{\widehat{EI}_z}{\widehat{EI}_y} - \frac{\widehat{GJ}}{4\widehat{EI}_y}\right)\frac{\pi}{L} & \frac{\widehat{EC}_w\pi^2}{4\widehat{EI}_yL^2} \\ 0 & -\left(1 - \frac{\widehat{EI}_z}{\widehat{EI}_y} - \frac{\widehat{GJ}}{4\widehat{EI}_y}\right)\frac{\pi}{L} & -\frac{Mo}{\widehat{EI}_y}\left(1 - \frac{\widehat{EI}_z}{\widehat{EI}_y}\right) & 0 \\ 0 & \frac{\widehat{EC}_w\pi^2}{4\widehat{EI}_yL^2} & 0 & 0 \end{bmatrix} \tag{17}$$

where $\widehat{EI}_y$ is the flexural stiffness, $\widehat{GS}_z$ and $\widehat{GS}_y$ are shear stiffnesses of a composite beam and e_z is the parameter of load height measured from the shear center [12].

The same procedure can be applied for different load conditions, modifying only the expression of the tangential matrix Kt, in fact redefining the elements of the matrix K_G, which consider the displacements due to the initial load. For example, in the case of a simply supported beam subjected to a distributed load q_z,

$$Kt = K + K_G q_z \tag{18}$$

where the tangential stiffness matrix is given in Box I:

6.2. Cantilever beams

In this case, the variational Eq. (8) is discretized by using beam characteristic orthogonal polynomials for the displacements v, θ_z, ϕ and θ, while the displacements w and θ_y (load plane) are adopted as the exact solution of the linearized problem. For this case, the only type of loading considered is a concentrated force applied at the free end of the beam. The corresponding expressions for the initial displacements are given by

$$w = -\frac{P}{\widehat{GS}_z}x + \frac{P}{\widehat{EI}_y}\left(\frac{x^3}{6} - L\frac{x^2}{2}\right);$$
$$\theta_y = \frac{P}{\widehat{EI}_y}\left(\frac{x^2}{2} - Lx\right). \tag{19}$$

$$K_G = \begin{bmatrix} 0 & 0 & 0 & 0 \\ & 0 & \left(\dfrac{6\widehat{GS}_y}{\pi L\widehat{GS}_z} - \dfrac{12(\widehat{EI}_z + \widehat{EI}_y) - 9\widehat{GJ}}{4\widehat{EI}_y\pi L} + \left(1 - \dfrac{\widehat{EI}_z}{\widehat{EI}_y} - \dfrac{\widehat{GJ}}{4\widehat{EI}_y}\right)\dfrac{\pi}{L}\right)\dfrac{L^2}{12} & -\dfrac{\widehat{EC}_w(\pi^2 - 9)}{48\widehat{EI}_y} \\ & -\dfrac{q_z}{\widehat{EI}_y}\left(1 - \dfrac{\widehat{EI}_z}{\widehat{EI}_y}\right)\dfrac{L^4}{\pi^4}\dfrac{(45 + \pi^4)}{120} - \dfrac{q_z}{\widehat{GS}_z}\left(1 - \dfrac{\widehat{GS}_y}{\widehat{GS}_z}\right)\dfrac{L^2}{\pi^2}\dfrac{(\pi^2 - 6)}{12} - e_z & 0 \\ Sym. & & & 0 \end{bmatrix}.$$

Box I.

The set of orthogonal polynomials which satisfy the geometrical boundary conditions are generated by using the Gram–Schmidt process.

$$U = \sum_{i=1}^{n} c_i \xi_i(x) \tag{20}$$

where U represents each of the displacements v, θ_z, ϕ and θ, and c_i are arbitrary coefficients which are to be determined. The polynomials $\xi_i(x)$ are generated as follows [17]:

$$\xi_2(x) = (x - B_2)\xi_1(x), \ldots, \xi_k(x)$$
$$= (x - B_k)\xi_{k-1}(x) - C_k\xi_{k-2}(x),$$

donde $B_k = \dfrac{\int_0^L x\xi_{k-1}^2(x)\mathrm{d}x}{\int_0^L \xi_{k-1}^2(x)\mathrm{d}x}$,

$$C_k = \frac{\int_0^L x\xi_{k-1}(x)\xi_{k-2}(x)\mathrm{d}x}{\int_0^L \xi_{k-2}^2\mathrm{d}x}. \tag{21}$$

The first member of the orthogonal polynomial $\xi_1(x)$ is chosen as the simplest polynomial (of the least order) that satisfies the boundary conditions.

$$\xi_1(x) : \begin{cases} 2xL & \text{corresponding to the displacements } v \text{ and } \phi. \\ \dfrac{2x}{L}(2L - x) & \text{corresponding to the displacements } \theta_z \text{ and } \theta. \end{cases} \tag{22}$$

6.3. Fixed-end beams

This case is similar to the previous one and it is necessary to find the expressions of the displacements corresponding to the load plane (w and θ_y). The generation of the orthogonal polynomials for the displacements v, θ_z, ϕ and θ, is carried out in the same way as that previously explained and the choice of the first term of the polynomial $\xi_1(x)$ is:

$$\xi_1(x) : \begin{cases} \left(\dfrac{x}{L}\right)^2 (L - x)^2 & \text{corresponding to the displacements } v \text{ and } \phi. \\ \dfrac{x}{L}(L - x) & \text{corresponding to the displacements } \theta_z \text{ and } \theta. \end{cases} \tag{23}$$

In order to obtain sufficiently accurate results, four terms ($n = 4$) are taken for each one of the flexural–torsional displacements. Due to the size of the resultant tangential matrix, it is difficult to obtain a simple expression and therefore one is not presented here.
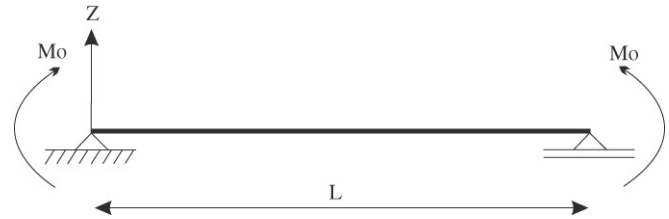

Fig. 2. Simply supported beam subjected to uniform moment.

7. Applications and numerical results

The purpose of this section is to apply the present theoretical model in order to study the free vibration behavior of thin-walled composite beams. In the tables and figures the following notation is used.

LF: denotes natural frequency values obtained from the classical or lineal theory, considering initial stresses and disregarding the initial deformation.

NLF: denotes natural frequency values obtained with this formulation, taking into account initial displacements.

On the other hand, the influence of shear deformation is analyzed for different laminate stacking sequence. In the following numerical results, the shear effect on the thickness $\gamma_{xn}^{(0)}$ has been neglected because its consideration conduces to inaccurate results for thin-walled sections, as explained by Piovan and Cortínez [8]. They showed that the inclusion of the in-thickness shear deformation effect erroneously increases the rigidity instead of flexibilizing the beam behavior.

7.1. Simply supported I-beam subjected to uniform moments

This example corresponds to a simply supported I-beam subjected to a uniform bending moment *Mo* applied about its major axis, as shown in Fig. 2. The geometrical properties are $h = 0.6$ m, $b = 0.6$ m, $e = 0.03$ m (Fig. 3). The analyzed material is graphite–epoxy (AS4/3501) whose properties are $E_1 = 144$ GPa, $E_2 = 9.65$ GPa, $G_{12} = 4.14$ GPa, $G_{13} = 4.14$ GPa, $G_{23} = 3.45$ GPa, $\nu_{12} = 0.3$, $\nu_{13} = 0.3$, $\nu_{23} = 0.5$, $\rho = 1389$ kg/m³.

The variation of the fundamental frequencies (Hz) as a function of the load parameter λ is shown in Figs. 4–6, for a sequence of lamination {*0/0/0/0*}, {*0/90/90/0*} and {*45/−45/−45/45*}, respectively. The moment load $M_0 = \lambda M_{cr}$

Table 1
Parameters in Eq. (24) and in Box II

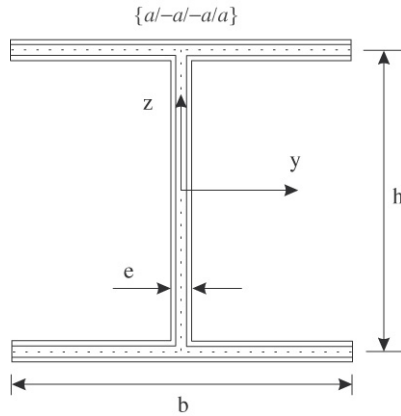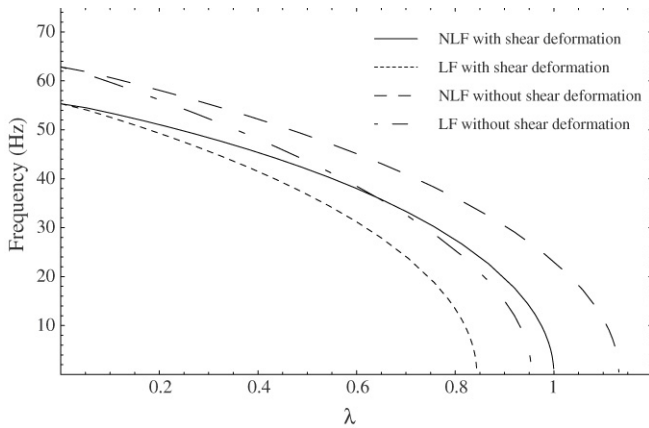| Simply supported beam	C1	C2	β	δ
(a) End moments	1	0	0.5	0
(b) Uniformly distributed load ($Mcr = q_z L^2/8$)	1.141	0.459	0.033	0.214
(c) Concentrated force ($Mcr = PL/4$)	1.423	0.554	0.076	0.083

Fig. 3. Analyzed cross-section shape.

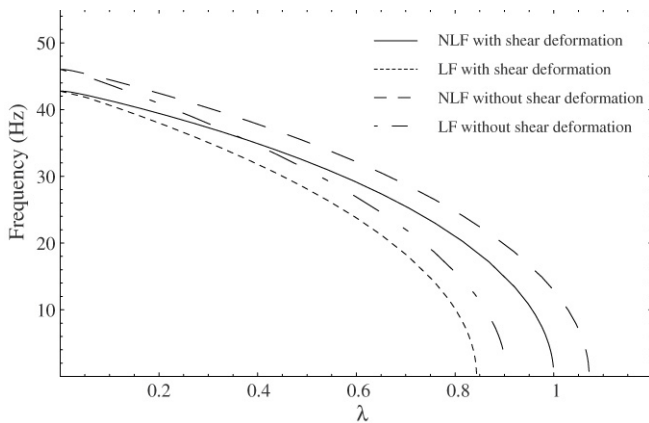Fig. 4. Natural frequencies of beams subjected to uniform bending, lamination {0/0/0/0}.

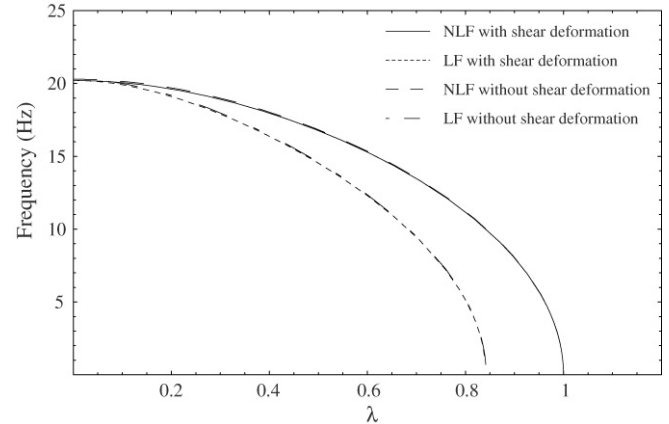Fig. 5. Natural frequencies of beams subjected to uniform bending, lamination {0/90/90/0}.

Fig. 6. Natural frequencies of beams subjected to uniform bending, lamination {45/−45/−45/ 45}.

is scaled with the value of the critical buckling load obtained by means of the formula developed by the authors in [12].

$$M_{cr} = C_1 \alpha \widehat{EI}_z \frac{\pi^2}{L^2} \left[-C_2 e_z \alpha \right.$$
$$\left. + \sqrt{\frac{\widehat{GS_w}\widehat{GJ} + \widehat{EC_w}\left(\widehat{GS_w} + \widehat{GJ}\right)\frac{\pi^2}{L^2}}{\widehat{EI}_z \frac{\pi^2}{L^2}\left(\widehat{GS_w} + \widehat{EC_w}\frac{\pi^2}{L^2}\right)} + (C_2 e_z \alpha)^2} \right]$$

(24)

where C_1, C_2, β and δ are approximate constants presented in Table 1, and α is defined in Box II.

The frequency values of the present formulation (NLF) and those obtained by disregarding the initial deflection (LF-classical Theory) are compared, analyzing in addition the influence of the shear deformation effect.

From the figures, it is possible appreciate that the effect of the bending moment is to decrease the fundamental frequency with respect to the unloaded case. The frequencies calculated from the linear analysis (LF) are smaller compared with those calculated from the non-linear model (NLF).

For example, for a load parameter $\lambda = 0.5$ and lamination {0/0/0/0}, the fundamental frequencies are:

- *Frequency* = 41.96 Hz, according to the present analysis (NLF).
- *Frequency* = 36.79 Hz, according to the classical analysis (LF).

The difference between both analyses can reach a percentage of about 12% and the effect of initial displacements becomes more significant as the load parameter λ increases. We observe

$$\alpha = \cfrac{1}{\sqrt{\left(1 - \dfrac{\widehat{EI}_z}{\widehat{EI}_y}\right)\left(1 - \beta\dfrac{\widehat{GJ}}{\widehat{EI}_y} - \beta\dfrac{\widehat{EC}_w\widehat{GS}_w\pi^2}{\widehat{EI}_y(\widehat{GS}_wL^2+\widehat{EC}_w\pi^2)}\right) - \delta\dfrac{\widehat{EI}_z}{\widehat{GS}_y}\dfrac{\pi^2}{L^2}\left[1 - \dfrac{\widehat{GS}_y}{\widehat{GS}_z}\left(0.71 - \dfrac{\widehat{GS}_y}{\widehat{GS}_z}0.29\right)\right]}}$$
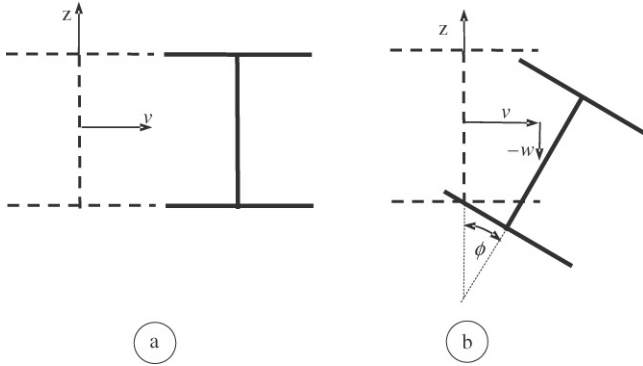
Box II.

Fig. 7. First flexural mode (a); *y* flexural–torsional mode (b).

that the effect of the initial deflections is important for all the sequences of lamination analyzed.

On the other hand, the shear deformation effect is significant for beams with unidirectional fibers and insignificant for the sequence of lamination {45/−45/−45/45}. For this last lamination the curves with and without shear deformation coincide for both NLF and LF analyses. The shear deformation may significantly reduce the natural frequency value, for example, for a load parameter $\lambda = 0.5$ and lamination {0/0/0/0}:

- *Frequency* = 41.96 Hz, according to *NLF with shear deformation*
- *Frequency* = 48.84 Hz, according to *NLF without shear deformation*.

This discrepancy can reach a percentage of about 16%, taking as reference the frequency value with shear deformation. Moreover, this effect keeps approximately constant as the load parameter is varied.

It is important to mention that in the case of $\lambda = 0$, the natural frequency corresponds to the first flexural mode (see Fig. 7(ⓐ)). Then, for any value of the load, the frequency corresponds to a flexural–torsional mode with initial deflection in the vertical direction (see Fig. 7(ⓑ)). The coupling between both modes is caused exclusively by the effect of the lateral load M_0.

It is interesting to observe that for a certain load parameter value, the natural frequency obtained with the present formulation coincides with that from the linear theory without shear deformation. This effect is observed for the lamination sequence {0/0/0/0} and {0/90/90/0}, and it is only presented for a certain load value, $\lambda \approx 0.65$ and $\lambda \approx 0.38$, respectively. Then, as we move away from this load value, the discrepancy among both theories becomes more noticeable.

7.2. Simply supported I-beam subjected to distributed load

In this example a simply supported I-beam under distributed load is considered for three load positions, as shown in Fig. 8. The load can be applied to the top flange (case ⓐ), at the shear center (case ⓑ), and to the bottom flange (case ⓒ). Attention is focused on the importance of the load height parameter effect on the dynamic behavior of the beam, considering the effect of the initial deformation. The geometrical properties and the analyzed material are the same as in the previous example.

Figs. 9–11 show comparative results between the non-linear (NLF) and linear (LF) dynamic analysis (considering shear effect) in function on the load parameter, for a sequence of lamination {0/0/0/0}, {0/90/90/0} and {45/−45/−45/45}, respectively. The load $q_z = \lambda q_{cr}$ is scaled with the value of the critical buckling load corresponding to the case ⓑ, by means of expression (24) and Box II. As in the previous case, the effect of the distributed load causes a reduction in the values of natural frequencies in relation to the unloaded state. Moreover, this decrease is more pronounced when the load is on the top flange, case ⓐ.

The load height parameter effect is smaller in the case of stacking sequence {45/−45/−45/45} in comparison with the other laminations. On the other hand, it is observed that the inclusion of initial deformation considerably increases the values of natural frequencies in comparison with the classical theory, as the load parameter increases. This effect is higher when the loads are on the bottom flange (case ⓒ) and for a lamination sequence {0/0/0/0}. When the load is applied in the shear center, this influence is similar to the one obtained in the previous example. Finally, in the three analyzed lamination sequences, it can be observed that when the load is on the top flange of the beam, the differences between both theories (NLF and LF) are smaller than in the other two load cases. For this I-beam the shear deformation effect continues to be important and has a similar behavior as in the previous example. For this reason, this effect is not discussed for this load condition.

7.3. Cantilever beam subjected to end force

The example considered is a cantilever I-beam subjected to an end force applied in the shear center; see Fig. 12. The analyzed material is the same as in the previous example and the geometrical properties of the beam are defined in Table 2. In this example the influence of the initial displacements on the dynamic behavior of a cantilever beam is studied, considering three different cross-sections and beams lengths. In Table 1, the natural frequencies values obtained with the present formulation (NLF) and those obtained from the classic theory (LF) are shown.
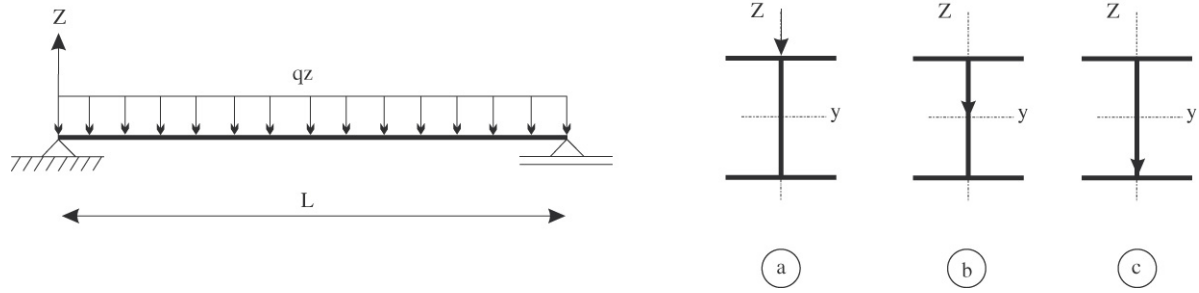
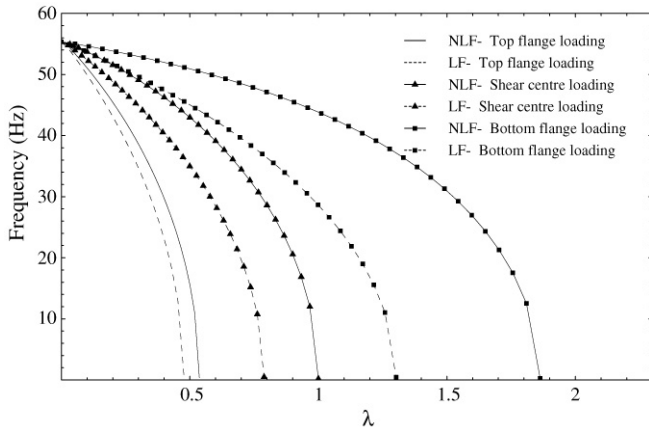Fig. 8. Different load heights.

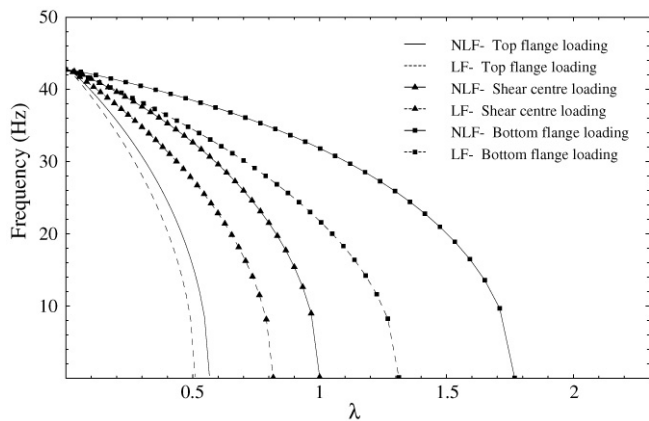Fig. 9. Natural frequencies versus load parameter, lamination {0/0/0/0}.

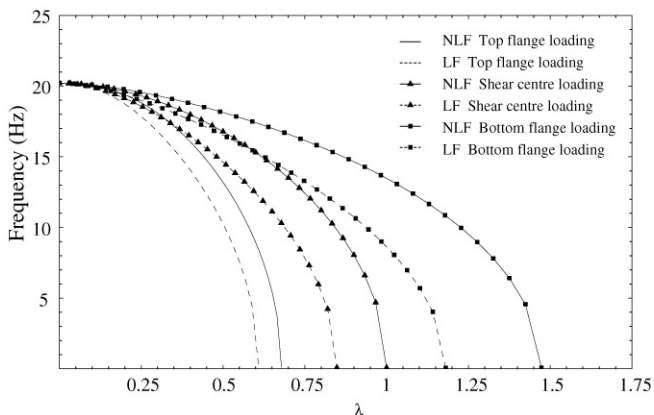Fig. 10. Natural frequencies versus load parameter, lamination {0/90/90/0}.

Fig. 11. Natural frequencies versus load parameter, lamination {45/−45/−45/45}.
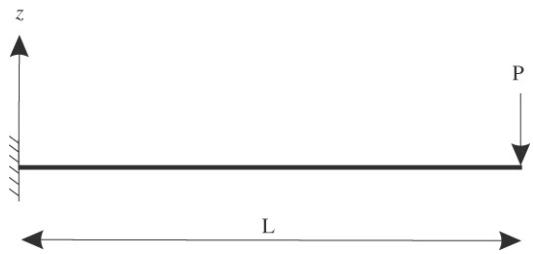

Fig. 12. Cantilever beam subjected to end force.

In all the cases, the concentrated load is scaled with the corresponding buckling load obtained as explained in [12], $P = \lambda P_{cr}$. The percentage difference between both theories is determined by taking as reference the values calculated with the present formulation (NLF).

The effect of the initial deformation, due to geometric non-linearity, is highly dependent on the relation between the bending stiffnesses $\widehat{EI}_z$ and $\widehat{EI}_y$. It is observed that the influence of the initial displacement is insignificant as the geometric relation $\widehat{EI}_z/\widehat{EI}_y$ decreases. For example, observing the first and second cross-section analyzed, the effect of the initial displacement is smaller when the flexural stiffness $\widehat{EI}_y$ increases, while $\widehat{EI}_z$ remains constant. Besides, this last effect is much smaller for the lamination sequence {0/90/90/0} in comparison with {0/0/0/0}, for the same load state.

7.4. Fixed-end beam subjected to concentrated force

A fixed-end I-beam loaded by a transverse force at the middle of the span is considered for three load positions, as shown in Fig. 13. The geometrical properties are $L = 12$ m, $h = 0.6$ m, $b = 0.6$ m and $e = 0.03$ m. The analyzed material is glass–epoxy (S2) whose properties are $E_1 = 48.3$ GPa, $E_2 = 19.8$ GPa, $G_{12} = 8.96$ GPa, $G_{13} = 8.96$ GPa, $G_{23} = 6.19$ GPa, $\nu_{12} = 0.27$, $\nu_{13} = 0.27$, $\nu_{23} = 0.6$, $\rho = 1389$ kg/m^3. The purpose of this section is to perform a comparison of the results obtained with the present formulation with those obtained from a shell finite elements model using Abaqus [18]. The beam is idealized by 240 four-node shell elements (S4). The analysis *STATIC is used in Abaqus as the first step of calculus, together with the option NLGEOM to consider the non-linear geometric effect in the pre-loaded state. Then, in the second step, the procedure *Frequency is used for the dynamic analysis of the structure.

Table 2
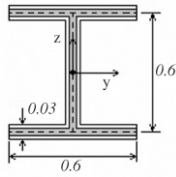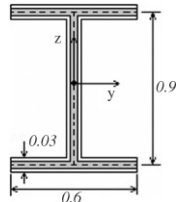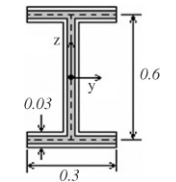Natural frequencies in Hz of a cantilever beam with the load applied in the shear center

Section	Lamination	Analysis	$L = 4$ m $\lambda = 0.6$	$L = 6$ m $\lambda = 0.8$	$L = 12$ m $\lambda = 0.9$
	{0/0/0/0}	NLF	28.04	10.44	2.77
		LF	14.84	6.05	2.20
		Difference	**47%**	**42%**	**21%**
	{0/90/90/0}	NLF	24.14	9.60	2.51
		LF	22.09	8.41	2.35
$\widehat{EI}_z/\widehat{EI}_y = 0.29$		Difference	**9%**	**12%**	**6%**
	{0/0/0/0}	NLF	30.45	11.04	2.61
		LF	25.20	7.51	2.26
		Difference	**17%**	**32%**	**13%**
	{0/90/90/0}	NLF	24.59	8.49	1.77
		LF	23.34	7.91	1.74
$\widehat{EI}_z/\widehat{EI}_y = 0.12$		Difference	**5%**	**7%**	**2%**
	{0/0/0/0}	NLF	17.67	6.30	1.41
		LF	17.42	6.21	1.39
		Difference	**1%**	**1%**	**1%**
	{0/90/90/0}	NLF	13.13	4.46	0.84
		LF	12.97	4.38	0.83
$\widehat{EI}_z/\widehat{EI}_y = 0.06$		Difference	**1%**	**1%**	**1%**

Table 3
Comparison of natural frequencies in Hz, fixed-end beam

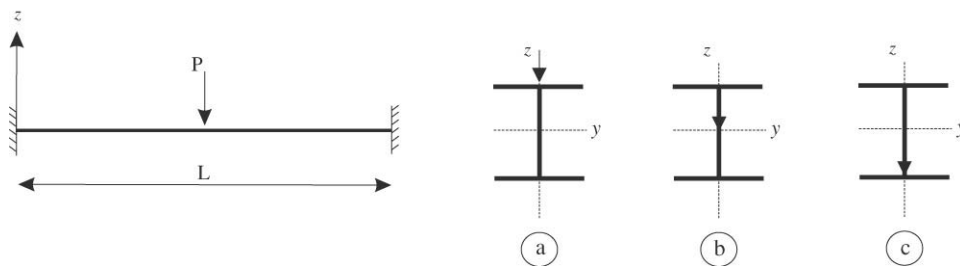| Lamination	Load condition		NLF	LF	Abaqus
{0/0/0/0}	$\lambda = 0$		20.17	20.17	19.95
	$\lambda = 0.5$	case ⓐ	15.09	14.74	14.96
		case ⓑ	15.18	14.66	15.83
		case ⓒ	18.41	14.41	18.91
{0/90/90/0}	$\lambda = 0$		17.10	17.10	16.96
	$\lambda = 0.5$	case ⓐ	12.99	12.72	12.97
		case ⓑ	12.98	12.58	12.81
		case ⓒ	13.02	12.31	14.33
45/−45/−45/45	$\lambda = 0$		14.73	14.73	14.70
	$\lambda = 0.5$	case ⓐ	11.76	11.57	11.93
		case ⓑ	11.47	11.20	11.45
		case ⓒ	11.26	10.75	12.71

Fig. 13. Fixed-end beam subjected to different load heights.

The concentrated load is scaled with the corresponding buckling load obtained as explained in [12], $P = \lambda P_{cr}$. The natural frequency values in Hz are shown in Table 3, for different load conditions and stacking sequences. The values
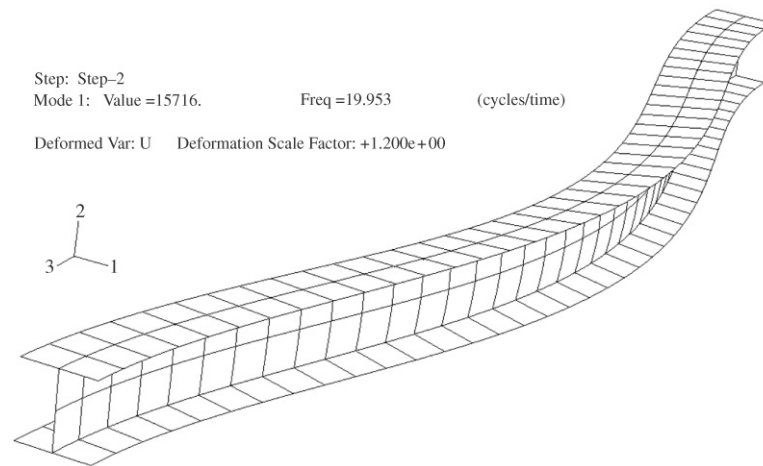
Step: Step–2
Mode 1: Value =15716.   Freq =19.953   (cycles/time)

Deformed Var: U   Deformation Scale Factor: +1.200e+00

Fig. 14. Flexural mode of a fixed-end unloaded beam, {*0/0/0/0*}.

Step: Step–2
Mode 1: Value = 8840.4   Freq =14.964   (cycles/time)

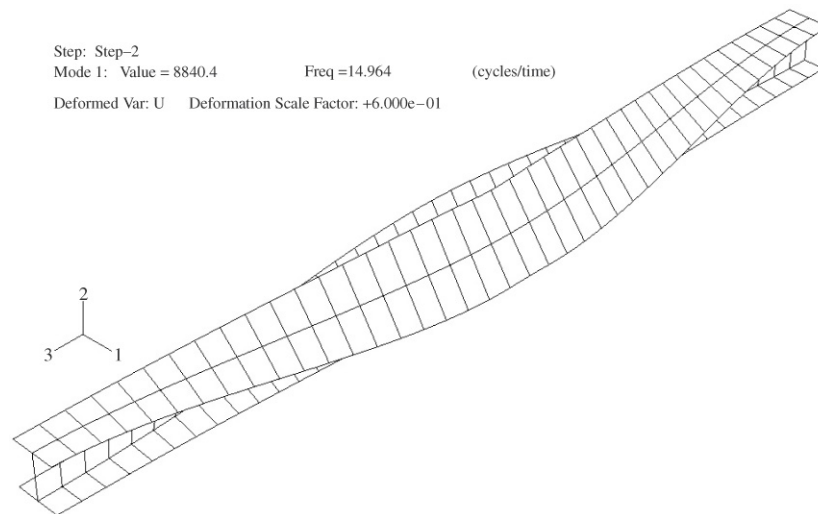Deformed Var: U   Deformation Scale Factor: +6.000e−01

Fig. 15. Flexural–torsional mode of a fixed-end beam subjected to initial load applied in the top flange, {*0/0/0/0*}.

obtained with the present formulation (NLF) are compared with those obtained with (LF) and those calculated with the shell finite elements model (Abaqus). In Figs. 14 and 15, the deformed configuration of the beam is shown, obtained with the program of finite elements (Abaqus) and considering a lamination {*0/0/0/0*}. This corresponds to the flexural unloaded mode (Fig. 14) and to the flexural–torsional mode with initial load applied in the top flange of the beam (Fig. 15).

The frequency values, corresponding to the pre-load state, obtained with the classic theory (LF) are always smaller in comparison with those that consider initial deflection (NLF and Abaqus). Also, the influence of the initial displacements is more important when the load is applied on the bottom flange of the beam and when the lamination sequence {*0/0/0/0*} is used. On the other hand, it is seen that the present solutions (NLF) are, in general, in good agreement with those obtained with Abaqus. When the loads are on the bottom flange of the beam, the values corresponding to the NLF model present a difference

from those obtained with Abaqus. This can be due partly to the fact that the dynamic response of the beam is more rigid than in the other load conditions and the finite elements solution presents some local modes associated to the global mode.

8. Conclusions

A one-dimensional model was developed for vibration analysis of composite thin-walled beams subjected to an initial state of stresses and deformations. The theory is formulated in the context of large displacements and rotations, through the adoption of a shear deformable displacement field (accounting for bending and warping shear) considering moderate bending rotations and large twist. The theory accounts for either open or closed bisymmetric cross-sections.

In particular, the influence of the initial deformation was studied on the dynamic response of a bisymmetric I-beam

subjected to end moments, concentrated forces, or uniformly distributed loads.

From the numerical examples studied, the natural frequencies obtained with the present analytical formulation (considering initial displacement effect) are in good agreement with those from finite element solutions. Based on the numerical results, the following conclusions are made:

- The vibration frequency values decrease as the initial load increases. Also, this decrease depends on the location of the load; for example, it is more pronounced when the load is applied in the top flange of the beam.
- Classical analysis of vibration may lead to inaccurate predictions due to the non-linear geometric effect increasing the frequency values. Moreover, the influence of this effect is higher as the load increases and consequently the initial displacements, corresponding to the load plane.
- The influence of the initial displacements on the dynamic behavior of the structure depends on the load position. In most of the cases, this effect is more important when the load is applied on the bottom flange of the beam.
- The lamination sequence also plays an important role on the dynamic behavior of the beam. The lamination sequence {*0/0/0/0*} presents a more stiff behavior than the other laminations.
- The relationship among the bending stiffnesses has great influence on the non-linear geometric effect. In the case of small values of the relation $\widehat{EI}_z/\widehat{EI}_y$ the influence of the initial deformation becomes insignificant, while for bigger values the influence becomes more important.
- For some laminations the shear deformation effect presents a great influence on the dynamic behavior of composite beams. The formulation without shear flexibility overestimates the values of natural frequency.

Acknowledgments

References

[1] Vlasov V. Thin walled elastic beams. Jerusalem: Israel Program for Scientific Translation; 1961.

[2] Bolotin V. The dynamic stability of elastic systems. San Francisco: HD; 1964.

[3] Coulter BA, Miller RE. Vibration and buckling of beam-columns subjected to non-uniform axial loads. Int J Numer Methods Eng 1986; 23:1739–55.

[4] Cortínez VH, Rossi RE. Dynamics of shear deformable thin-walled open beams subjected to initial stresses. Rev Internac Métod Numér Cálc Diseñ Ingr 1998;14(3):293–316.

[5] Kim SB, Kim MY. Improved formulation for spatial stability and free vibration of thin-walled tapered beams and space frames. Eng Struct 2000; 22:446–58.

[6] Jun L, Hongxing H, Rongying S, Xianding J. Dynamic response of axially loaded monosymmetrical thin-walled Bernoulli–Euler beams. Thin-Walled Struct 2004;42:1689–707.

[7] Mohri F, Azrar L, Potier-Ferry M. Vibration analysis of buckled thin-walled beams with open sections. J Sound Vib 2004;275:434–46.

[8] Cortínez VH, Piovan MT. Vibration and buckling of composite thin-walled beams with shear deformability. J Sound Vib 2002;258(4):701–23.

[9] Jun L, Rongying S, Hongxing H, Xianding J. Bending–torsional coupled dynamic response of axially loaded composite Timosenko thin-walled beam with closed cross-section. Compos Struct 2004;64:23–35.

[10] Timoshenko SP, Gere JM. Theory of elastic stability. 2nd ed. New York: McGraw-Hill; 1961.

[11] Sapkás A, Kollár LP. Lateral-torsional buckling of composite beams. Int J Solids Struct 2002;39:2939–63.

[12] Machado SP, Cortínez VH. Lateral buckling of thin-walled composite bisymmetric beams with prebuckling and shear deformation. Engineering Structures 2005;27:1185–96.

[13] Barbero EJ. Introduction to composite material design. Taylor and Francis Inc; 1999.

[14] Reddy JN. Mechanics of laminated composite plates and shells: Theory and analysis. 2nd ed. Boca Raton (FL): CRC Press; 2004.

[15] Reddy JN. Energy principles and variational methods in applied mechanics. 2nd ed. NY: John Wiley; 2002.

[16] Washizu K. Variational methods in elasticity and plasticity. Pergamon Press; 1968.

[17] Bhat RB. Transverse vibrations of a rotating uniform cantilever beam with tip mass as predicted by using beam characteristic orthogonal polynomials in the Rayleigh–Ritz method. J Sound Vib 1986;105(2):199–210.

[18] Abaqus standard user's manual, v. 5.6. Pawtucket (RI): Hibbit Karlsson and Sorensen, Abaqus, 1999.